

## Evaluation of the prognostic value of lateral MAPSE in patients with suspected coronary artery disease

Chengxi Yan<sup>a</sup>, Ying Chang<sup>b</sup>, FangWu<sup>c</sup>, Minglei Yang<sup>d</sup>, Shuangfeng Dai<sup>d</sup>, Jiannan Zhang<sup>a</sup>, Yuelang Zhang<sup>a,\*</sup>

<sup>a</sup> Department of Radiology, The Second Affiliated Hospital of Xi'an Jiaotong University, Xi'an, China

<sup>b</sup> Department of Ultrasound, Xuanwu Hospital, Capital Medical University, Beijing, China

<sup>c</sup> Department of Radiology, Xuanwu Hospital, Capital Medical University, Beijing, China

<sup>d</sup> Beijing Wandong Medical Technology Ltd., Beijing, China

### ARTICLE INFO

#### Keywords:

Cardiovascular magnetic resonance  
Prognosis  
Coronary artery disease  
Mitral annular plane systolic excursion  
Follow up

### ABSTRACT

**Objectives:** To evaluate the prognostic value of lateral mitral annular plane systolic excursion (MAPSE) in the prediction of major adverse cardiology events (MACE) in patients with suspected coronary artery disease (CAD). **Methods:** 233 consecutive patients were enrolled with suspected CAD from October 2012 to September 2013 and performed contrast-enhanced cardiac magnetic resonance (CMR) and two-dimensional echocardiogram studies no later than 72 h after admission. CMR imaging protocol included 4-chamber cine(cine-CMR), cardiovascular magnetic resonance angiography (CMRA) and late gadolinium enhancement (LGE). The primary endpoint is the time of first occurrence of a MACE. The independent association between lateral MAPSE and MACE was evaluated by Kaplan-Meier analysis and multivariable Cox regression analysis. C statistic and net reclassification improvement (NRI) were used to evaluate the prognostic value of lateral MAPSE in MACE. **Results:** Forty-five MACE occurred during an average follow-up of 9.2 years. Patients with lateral MAPSE < 9.885 mm experienced a significantly higher incidence of MACE than patients with lateral MAPSE  $\geq$  9.885 mm ( $P < 0.001$ ). After adjustment for established univariate predictors (age, diabetes, hypertension, hypercholesterolemia, transmural myocardial infarction), lateral MAPSE remained a significant independent predictor of MACE (HR = 1.373;  $P = 0.020$ ). The incorporation of lateral MAPSE into the risk model resulted in significant improvement in C statistic (increasing from 0.668 to 0.844;  $P = 0.005$ ). NRI improvement was 0.33 ( $P < 0.001$ ). **Conclusions:** lateral MAPSE derived from cine-CMR is an independent predictor of MACE, and improve risk reclassification beyond traditional clinical and CMR risk factors in patients with suspected coronary disease.

### 1. Introduction

Coronary artery disease (CAD) has been on the rise as a cause of mortality across the world. Primary prevention is key to limit the burden of CAD and relies on management of risk factors and healthy lifestyle [1]. Cardiac magnetic resonance (CMR) is uniquely able to assess for the presence of coexisting nonischemic etiologies in patients with a history of CAD, and CMR is accurate and cost-effective for diagnosis and risk stratification in patients with suspected CAD [2].

Recently studies demonstrated that the mitral annular plane systolic excursion (MAPSE) has been suggested as a parameter for left ventricular (LV) function, and the current clinical application and potential implications of routinely using MAPSE in patients with various

cardiovascular diseases [3]. Reduced MAPSE reflects impaired longitudinal function and thus provides complementary information to ejection fraction (EF), which represents the global result of both longitudinal and circumferential contraction [4]. MAPSE has been shown to be a major contributor to left ventricular pumping in both health and disease played a fundamental role in cardiac mechanics and appears to be an early marker for a number of pathological states. Moreover, MAPSE is independent of image quality since its measurement only requires visualization of the mitral annulus without delineation of the left ventricular (LV) endocardial boundary. Usually, MAPSE can be measured from two long-axis views, four- and two-chamber view, but in general, it should be extracted from septal and lateral mitral annulus [5,6]. While right ventricular dysfunction can affect the measurement of septal

\* Corresponding author.

E-mail address: [zhyl003@163.com](mailto:zhyl003@163.com) (Y. Zhang).

<https://doi.org/10.1016/j.ijcha.2024.101567>

Received 22 October 2024; Received in revised form 16 November 2024; Accepted 20 November 2024

2352-9067/© 2024 The Authors. Published by Elsevier B.V. This is an open access article under the CC BY-NC-ND license (<http://creativecommons.org/licenses/by-nc-nd/4.0/>).

MAPSE, lateral MAPSE is more sensitive and specific for measuring the global longitudinal function of the LV [7]. The assessment of lateral MAPSE using cardiac magnetic resonance (CMR) has shown to provide short-term prognostic value in an unselected cohort with suspected cardiac disease [8,9]. However, the long-term prognostic value of MAPSE in patients with suspected CAD is still unknown so far.

Therefore, the aim of this paper was to examine the current and recently available evidence on MAPSE as a marker of cardiac function, and to highlight that lateral MAPSE may have good long-term prognostic value in patients with suspected CAD. Firstly, 233 patients with suspected of CAD were enrolled in this study from October 2012 to September 2013, followed for more than 9 years, and made the MACE as the end event. Then the independent association between lateral MAPSE and MACE was evaluated by Kaplan-Meier analysis and multivariable Cox regression analysis. C statistic and net reclassification improvement (NRI) were used to evaluate the prognostic value of lateral MAPSE in MACE. The results of data analysis verified the prognostic value of lateral MAPSE in patients with suspected CAD.

## 2. Methods

### 2.1. Study population

The study population consisted of 233 consecutive patients who presented to our outpatient clinic or were admitted to our hospital for cardiac evaluation (electrocardiogram, echocardiography, or invasive coronary angiography) from October 2012 to September 2013 because of suspected CAD (elevated risk profile, new-onset chest pain, abnormal stress test). All subjects have consented to participate in this study. This research was approved by the Institutional Ethics Committee for Human Research at Xuanwu Hospital (Beijing, China). Exclusion criteria for this contrast-enhanced whole heart CMR study were (a) prior CAD, including prior MI, CAD on prior revascularization, (b) hemodynamic instability, (c) contraindication to CMR.

### 2.2. Image acquisition

#### 2.2.1. CMR imaging

All the patients underwent scanning using 3.0 T magnetic resonance imaging scanner (MAGNETOM Trio, A Tim System; Siemens AG Healthcare, Erlangen, Germany). Detailed imaging-acquisition methods have previously described [10]. After initial localizers, retrospective ECG-triggered cine imaging (50 cardiac phases reconstructed) was performed in a single four-chamber view using a fast low-angle shot (FLASH) sequence during free breathing.

For whole-heart coronary magnetic resonance angiography (CMRA), intravenous gadolinium contrast (0.2 mmol/kg body weight of Gadobenate Dimeglumine) was slowly infused using a power injector. 60 s later, CMRA data acquisition was started. Imaging volume was prescribed in the axial plane to cover the entire heart in the axial (TR/TE = 3.0/1.4 ms, flip angle = 20°, readout bandwidth = 610 Hz/pixel, acquired voxel size = 1.3\*1.3\*1.7 mm<sup>3</sup>).

15 min later after the initiation of contrast administration, a series of short axis slices (8–10, typically) LGE images, from base to apex covering the entire left ventricle, were acquired using phase sensitive inversion recovery technique.

#### 2.2.2. Echocardiography

Echocardiography was performed using EPIQ7 machines (Philips Ultrasound, US). 2D parasternal long axis view including the apex and short-axis views obtained at the level of the mitral valve (basal LV level), papillary muscles (papillary level), and apex (apical level).

### 2.3. Image analysis

#### 2.3.1. Analysis of CMRA images

For postprocessing, certified specific software (CVI 42, version 5.1.1, Circle Cardiovascular Imaging) was applied. CMR images were assessed by two experienced readers (cardio-radiologists) who blinded to the patient's information and performed the measurements in consensus. Axial source images, curved multiplanar reformations (MPR), and thin-slab maximum-intensity projections (MIP) images were used to determine the presence or absence of significant luminal narrowing ( $\geq 50\%$  diameter reduction) of entire coronary arteries on whole-heart CMRA.

#### 2.3.2. MAPSE assessment

The systolic MAPSE should be measured from the lowest point at end-diastole to the end-systole (just before mitral valve opening) in a single 4-chamber view. Septal MAPSE was defined as the simple linear distance of septal attachment of mitral annular plane from end-diastole to the end-systole. Similarly, lateral MAPSE was defined as the distance of lateral attachment of mitral valve between end-diastole and end-systole (Fig. 1).

#### 2.3.3. Analysis of LGE images

LGE Images were evaluated qualitatively for the presence or absence. Volume fraction of LGE was calculated using a threshold of 5SD above the signal intensity of remote myocardium [11] by semiautomatically determined with manual correction. When extension of enhancement myocardial was 50% or more of the transmural distance, we defined it as transmural myocardial infarction (TMI) [12].

#### 2.3.4. Analysis of echocardiography images

Left ventricular ejection fraction (LVEF) was obtained by hemispheroid-cylinder model. Combined figure model in which the LV is divided into cylinder and hemi ellipsoid.

The volume is calculated from the formula  $\text{Volume} = 5/6AL$ : Where A is LV cavity area at the level of papillary muscles and L length of the LV. The LVEF was then calculated according to formula:

$$\text{LVEF} = \frac{\text{EDV} - \text{ESV}}{\text{EDV}} \times 100\%$$

where EDV is end diastolic volume and ESV is the end systolic volume.

### 2.4. Follow-up

Patients were followed for the combined primary outcome of MACE-cardiac death, non-fatal myocardial infarction, hospitalization for unstable angina, and late revascularization (>30 days after CMR). Two cardiologists blinded to CMR results performed all standardized follow-up procedures. Follow-up obtained via telephone interview, electronic medical records. For cases whose records were not found in medical chart, treating physicians and patients were contacting using a standardized questionnaire. Time to event was calculated as the period between the CMR study and first occurrence of a MACE. The follow-up was ceased in November 2022.

### 2.5. Statistical methods

SPSS Statistics (version 21.0; IBM Corp, Armonk, NY, USA) and GraphPad Prism (6.0; GraphPad Software Inc., La Jolla, CA, USA) were used for statistical analysis. Normally distributed data were expressed as mean  $\pm$  SD. Categorical variables are expressed as absolute numbers and percentages. Continuous variables were compared by Student's *t*-test. Chi-square was used to compare the discrete variables. A linear regression and Bland-Altman analysis was used to detect inter observer variability. To evaluate time to primary outcomes of MACE, the Kaplan-Meier was applied. All variables were evaluated using univariate Cox

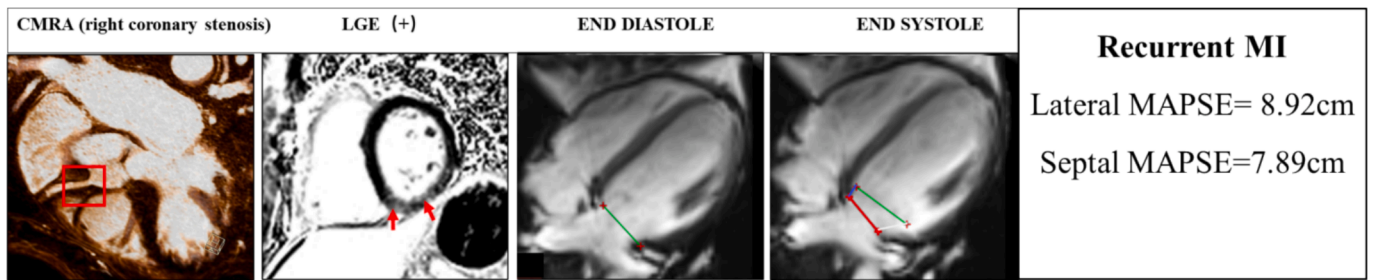


**Fig. 1.** Demonstrate measurement of MAPSE in a patient who had right coronary stenosis and recurrent myocardial infarction (MI) 3 years after the CMR exam. (A) Left anterior oblique whole-heart CMRA preformatted with curved multiplanar reformation shows significant luminal narrowing (red rectangle) in the proximal part of the RCA. (B) CMR late gadolinium hyperenhancement slices of left ventricular short axis showing MI in inferior zones (red arrow). (C-D) Septal and lateral mitral annular positions were recorded at end diastole (red line) and end systole (green line), allowing for assessment of lateral (white line) and septal MAPSE (blue line). In 20 randomly selected patients, a second blinded CMR physician measured MAPSE for assessment of interobserver variability.

proportional hazards regression modeling to identify their prognostic power in predicting MACE. Hazard ratios (HRs) with corresponding 95 % confidence intervals (CIs) were obtained. All significant univariate predictors ( $P < 0.05$ ) were then entered into multivariate Cox model to ascertain their significant multivariate predictors. C-statistics were used to compare model discrimination as well as the integrated discrimination improvement, which provides a measure of improvement in sensitivity and specificity of the model with addition of new predictor (MAPSE) [13]. Risk reclassification analysis was performed with reclassification improvement (NRI) by using categories of  $< 6\%$ ,  $6\text{--}20\%$ ,  $> 20\%$  10-year coronary heart disease risk to define low, intermediate, and high-risk categories, respectively [14].

### 3. Results

#### 3.1. Patient characteristics

Of the 233 patients initially enrolled, 203 patients had complete CMR data for further MAPSE assessment. A total of 106 patients with significant stenosis underwent revascularization (percutaneous coronary intervention ( $n = 92$ ), bypass surgery ( $n = 14$ ) within 30 days after CMR. After an average follow-up of 9.2 years, 189 patients were included and revealed a MACE in 45 (cardiac death,  $n = 7$ ; non-fatal myocardial infarctions,  $n = 18$ ; hospitalization for unstable angina,  $n = 12$ ; late coronary revascularization,  $n = 8$ ) (Fig. 2).

Baseline patient characteristics stratified by a coronary artery stenosis grade above and below 50 % were summarized in Table 1. Mean age of the study population was  $55 \pm 9.93$  years. TMI was only occurred in patients with significant coronary stenosis. Moreover, there was a significant higher percentage of male, older patients, and smokers in the individuals with significant coronary stenosis. Patients without significant coronary stenosis had higher LVEF than those of patients with significant coronary stenosis, ( $62.41\% \pm 11.32$  vs.  $50.21 \pm 11.43$ ,  $P < 0.001$ ). Besides, both lateral MAPSE and septal MAPSE were significantly higher in patients without significant coronary artery stenosis (lateral MAPSE,  $11.69 \pm 3.25$  vs.  $9.84 \pm 3.53$ ,  $P < 0.001$ ; septal MAPSE,  $10.32 \pm 2.85$  vs.  $9.26 \pm 2.41$ ,  $P = 0.005$ ).

#### 3.1.1. Determinants of MACE

In univariate Cox proportional hazard regression models, the following variables were shown to predict increased rate MACE: hypertension (HR, 2.909; 95 %CI, 0.207–2.140;  $P = 0.022$ ), hypercholesterolemia (HR, 3.782; 95 %CI, 1.562–9.161;  $P = 0.003$ ), heart rate (HR, 1.057; 95 %CI, 1.005–1.111;  $P = 0.031$ ), LGE% (HR, 0.958; 95 %CI, 0.925–0.991;  $P = 0.007$ ), TMI (HR, 4.000; 95 %CI, 1.921–8.382;  $P = 0.000$ ), lateral MAPSE (HR, 1.423; 95 %CI, 1.256–1.612;  $P = 0.000$ ) and septal MAPSE (HR, 1.423; 95 %CI, 1.256–1.612;  $P = 0.000$ ) (Table 2).

After adjustment for established clinical and CMR risk factors which were univariate predictors (hypertension, hypercholesterolemia, heart

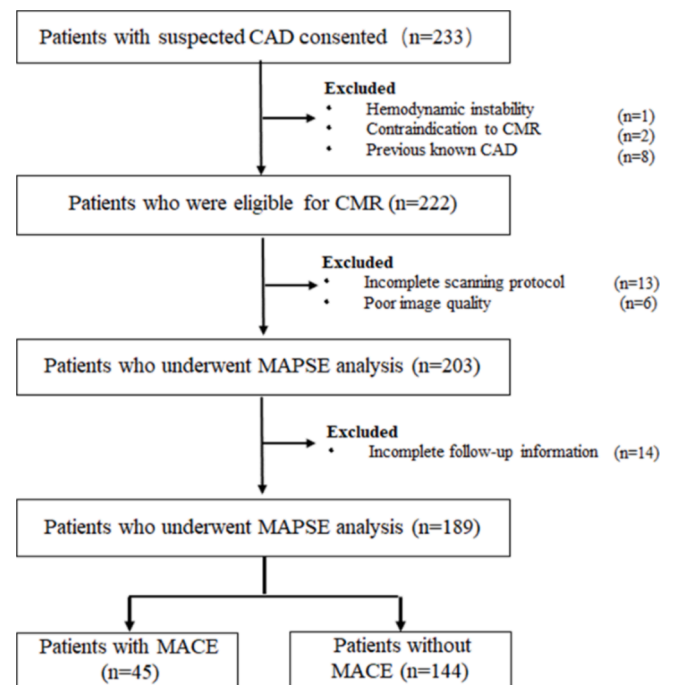


**Fig. 2.** Study inclusion flowchart. CAD = coronary artery disease, CMR = cardiac magnetic resonance, MAPSE = mitral annular plane systolic excursion, MACE = major adverse cardiac event.

rate, LGE%, TMI and septal MAPSE), lateral MAPSE remained a significant independent predictor of MACE (HR, 1.3731; 95 %CI, 1.051–1.794;  $P = 0.020$ ) (Table 2).

#### 3.1.2. Incremental prognostic value of lateral MAPSE

Cox proportional hazard analysis with the C-statistics were used to assess the incremental prognostic value of lateral MAPSE for the MACE, as shown in Table 3. Adding the lateral MAPSE to hypercholesterolemia, TMI, resulted in an increase in C-statistics of 0.156 ( $P = 0.005$ ). Besides, in significant stenosis, adding lateral MAPSE to hypercholesterolemia, TMI, resulted in an increase in C-statistics of 0.166 ( $P = 0.013$ ). However, there is no incremental prognostic value when adding lateral MAPSE to hypercholesterolemia, TMI in non-significant stenosis group, with the  $P$  value = 0.215. Overall, the net reclassification improvement (NRI) was 0.33 ( $p = 0.000$ ) across risk categories of MACE. When stratified by coronary stenosis, adding the lateral MAPSE significantly improved the NRI for those with significant coronary stenosis with the value of 0.39 ( $P = 0.001$ ), however, it can't improve the NRI in patients without significant coronary stenosis,  $P = 0.09$ .

**Table 1**  
Baseline characteristics for study population.

Variable	All Study Participants (n = 189)	No Significant Stenosis (n = 83)	Significant Stenosis (n = 106)	P Value
<b>Sex</b>				
Male	121 (64.02 %)	40 (48.19 %)	81 (76.42 %)	<0.001
Female	68 (35.98 %)	43 (51.81 %)	25 (23.58 %)	<0.001
Age (y)*	55 ± 9.93	56.91 ± 9.92	60.15 ± 9.95	0.026
Body mass index (kg/m <sup>2</sup> )*	24.3 ± 2.77	24.28 ± 2.96	24.14 ± 2.09	0.505
<b>Cardiovascular risk factor</b>				
Hypertension	88 (46.56 %)	36 (43.37 %)	52 (49.06 %)	0.437
Smoking	56 (29.63 %)	16 (19.28 %)	40 (37.73 %)	0.005
Hypercholesterolemia	33 (17.46 %)	18 (21.69 %)	15 (14.15 %)	0.230
Diabetes mellitus#	32 (16.93 %)	10 (12.05 %)	22 (20.07 %)	0.113
Heart rate (beat/min)*	66.61 ± 11.07	67.96 ± 10.28	65.43 ± 11.67	0.361
LVEF%*	57.62 ± 10.59	62.41 ± 11.32	50.21 ± 11.43	<0.001
LGE present	63 (33.33 %)	2 (2.4 %)	61 (57.5 %)	<0.001
LGE%	4.95 ± 9.12	0.69 ± 3.98	7.64 ± 10.24	<0.001
TMI	45 (23.81 %)	0	45 (42.45 %)	<0.001
Lateral MAPSE (cm)*	10.57 ± 3.45	11.69 ± 3.25	9.84 ± 3.53	<0.001
Septal MAPSE (cm)*	9.87 ± 2.62	10.32 ± 2.85	9.26 ± 2.41	0.005

Note: Unless otherwise specified, data are the number of participants, with percentages in parentheses.

\* Date are means ± standard deviation.

# Diabetes mellitus was defined as a history of diet-controlled or treated diabetes.

MAPSE = mitral annular plane systolic excursion, LGE = late gadolinium enhancement, LVEF = left ventricular ejection fraction.

### 3.1.3. Outcomes stratified by MAPSE

Receiver operating characteristics (ROC) analysis revealed area under curve (AUC) of lateral MAPSE was 0.815 (95 %CI, 0.739–0.890;  $P = 0.000$ ) with the optimal cut-off value 9.885 mm as shown in Fig. 3. By Kaplan-Meier analysis, patients with lateral MAPSE < 9.885 mm experienced significantly higher incidence of MACE than patients with lateral MAPSE ≥ 9.885 mm (log-rank  $P = 0.000$ ) (Fig. 4). Those patients whose lateral MAPSE < 9.885 mm and coronary stenosis > 50 % experience highest cumulative incidence of MACE, as shown in Fig. 5.

### 3.1.4. Inter observer variability of lateral MAPSE

Linear regression and Bland-Altman analysis were used to determine the inter observer variability of lateral MAPSE. Linear regression analysis showed a high correlation between the two observers with  $R^2 = 0.92$  (Fig. 6a). Bland-Altman showed a bias of 0.059 mm and limits of agreement were -1.933 to 2.050 mm (Fig. 6b).

## 4. Discussion

To the best of our knowledge, this is the first study to assess the long-term (9 years) prognostic value of MAPSE in the prediction of MACE in patients with suspected CAD. The result in current study indicated that lateral MAPSE derived from cine images is a powerful, independent predictor of MACE at long-term follow up. Simultaneously assess extent

**Table 2**  
Univariable and Multivariable Predictors of MACE.

Variable	Univariable		Multivariable	
	Hazards Ratio (95% CI)	P value	Hazards Ratio (95% CI)	P value
Male	1.228 (0.597–2.527)	0.577	—	—
Age	0.974 (0.940–1.008)	0.089	—	—
Body mass index	1.062 (0.903–1.248)	0.466	—	—
Hypertension	2.909 (0.207–2.140)	0.022	2.1 (0.498–8.852)	0.312
Smoking	1.403 (0.629–3.127)	0.408	—	—
Hypercholesterolemia	3.782 (1.562–9.161)	0.003	5.105 (1.203–21.675)	0.027
Diabetes mellitus	2.255 (0.932–5.455)	0.071	—	—
Heart rate	1.057 (1.005–1.111)	0.031	1.063	0.092
LVEF	1.082 (0.981–1.865)	0.051	—	—
LGE%	0.958 (0.925–0.991)	0.007	1.067	0.337
TMI	4.000 (1.921–8.382)	0.000	14.805 (1.275–71.961)	0.031
Lateral MAPSE	1.423 (1.256–1.612)	0.000	1.373 (1.051–1.794)	0.020
Septal MAPSE	1.448 (1.234–1.699)	0.000	1.128 (0.798–1.594)	0.495

Note: Unless otherwise specified, data are means ± standard deviations. Abbreviation is as in Table 1.

of myocardial infarction, coronary stenosis and MAPSE in one CMRA scanning would help to stratify patients with suspected CAD who are at risk for MACE.

Moreover, when dividing patients into two groups based on the coronary stenosis, the results seemed different for this simple parameter can't provide prognostic information incremental to common clinical and imaging risk factors in patients without significant coronary stenosis while showed the opposite results in the other group. Thus, these findings have potentially broad application to patients with significant coronary stenosis.

Even though, coronary CT angiography was one of the most robust technique for noninvasive visualization of coronary arteries [15–17], and has been validated against conventional coronary angiography [18], CMRA still has several advantages over coronary CT angiography [10,19]. First, it doesn't expose patients to ionizing radiation. Besides, for some heavy coronary artery calcification that can't visualize on coronary CT angiography due to blooming artifact, CMRA has advantages over [20]. The diagnostic value of CMRA has been invested in previous studies with a sensitivity of 78 %-96 % and a specificity of 68 % to 96 % in the patients with significant coronary artery stenosis which was identified at conventional angiography [10,21,22]. For the prognostic value of CMRA, it has been highlighted by Yeonyee et al, who used CMRA to visualize coronary lumen, and finally found that after a median follow-up of 25 months, patients with coronary stenosis experienced significantly more cardiac event with the annual event rate of 6.3 % than those without coronary stenosis with the annual rate of 0.3 % [23]. On our study, we also found that higher cardiac event rate existed in significant coronary stenosis group with an incidence rate of 33.13 % compared with other group with the incidence rate of 11.32 %.

The presence of LGE is a powerful prognostic marker of various cardiovascular disease [24,25]. Its absence seemed to provide the assurance of patients who were suspected at high risk of cardiac event [26]. LGE can accurately assess irreversible myocardial injury for its tissue resolution is superior to other technique such as single emission computed tomography (SPECT) imaging [27]. Myocardial scar on LGE

**Table 3**  
C Statistics for Cox Proportional Hazard Models to Predict MACE.

Variable	All Study Participants (n = 189)			Significant Stenosis (n = 106)			No Significant Stenosis (n = 83)		
	C-statistics (95 % CI)	Increment in C-statistics	P value	C-statistics (95 % CI)	Increment in C-statistics	P value	C-statistics (95 % CI)	Increment in C-statistics	P value
Lateral MAPSE	0.815 (0.739–0.899)			0.830 (0.746–0.915)			0.719 (0.539–0.899)		
TMI	0.639 (0.540–0.737)			0.635 (0.518–0.752)					
Lateral MAPSE + TMI	0.821 (0.756–0.895)	0.182	0.000	0.844 (0.767–0.921)	0.209	0.002			
Hypercholesterolemia	0.590 (0.489–0.690)			0.600 (0.476–0.724)			0.644 (0.415–0.873)		
Lateral MAPSE + Hypercholesterolemia	0.811 (0.734–0.888)	0.221	0.001	0.856 (0.780–0.931)	0.256	0.000	0.789 (0.623–0.955)	0.145	0.316
TMI + Hypercholesterolemia	0.688 (0.595–0.781)			0.697 (0.585–0.809)					
Lateral MAPSE + TMI + Hypercholesterolemia	0.844 (0.776–0.912)	0.156	0.005	0.863 (0.795–0.923)	0.166	0.013			

<sup>a</sup>This manuscript is the authors’ original work and has not been published nor has it been submitted simultaneously elsewhere.

<sup>b</sup>All authors have checked the manuscript and have agreed to the submission.

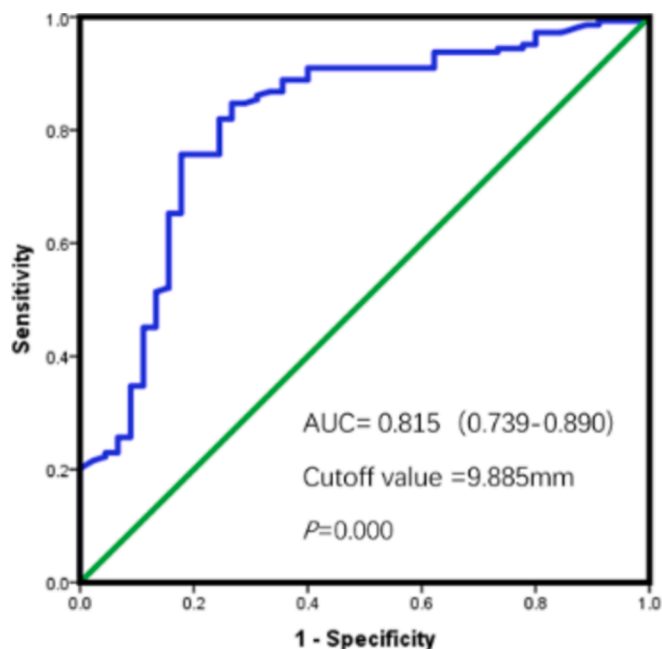


**Fig. 3.** Receiver-operator characteristic curves of Lateral MAPSE.

may indicated a poor response to beta-blocker therapy, or revascularization surgery [28]. The Transmural myocardial infarction depicted on LGE showed a close relationship with spontaneous ventricular arrhythmia in patients with CAD and implantable cardioverter defibrillators [29]. Myocardial fibrosis can not only reduce the overall myocardial contractility, but also contribute to ventricular arrhythmias that might lead to sudden cardiac death [29–31]. In addition, patients without clinical evidence of myocardial infarction while showed LGE on CMR still inflict significant morbidity and mortality [32,33]. Our study supported a previous study which elaborated that in LGE size wasn’t a significant predictor of MACE, and added to the increasing evidence that the presence of transmural myocardial infarction expressed by LGE had deleterious effects in cardiovascular disease with the highest hazard ratio value.

MAPSE plays a fundamental role in cardiac pump function, and usually measured from two long-axis views, four-and two-chamber view [34], but in general, it should be extracted from septal and lateral mitral annulus [35]. It was regarded as a surrogate of ventricular long-axis

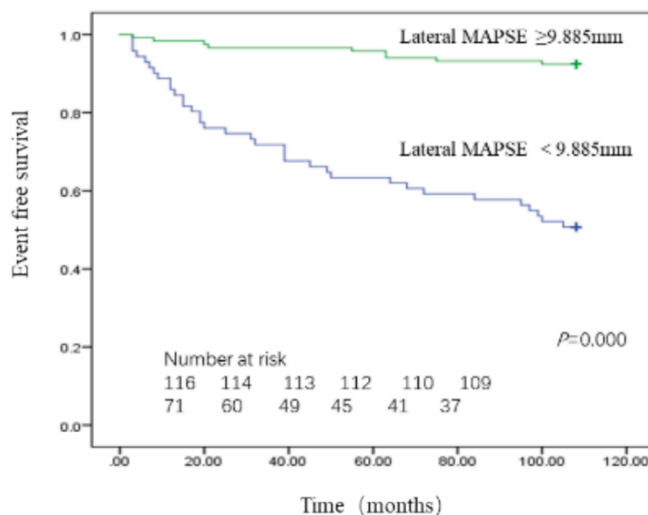


**Fig. 4.** Kaplan-Meier curves for MACE, in patients with lateral MAPSE above and below 9.885 mm.

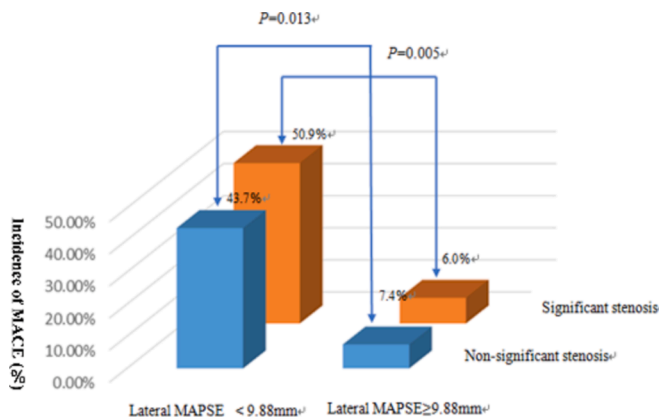


**Fig. 5.** Overall incidence of MACE stratified by lateral MAPSE and coronary stenosis.

function for cardiac apex was fixed with chest wall, by measuring changes of mitral position, long-axis function can be assessed [36]. While, the exactly causes of long axis function injured haven’t been

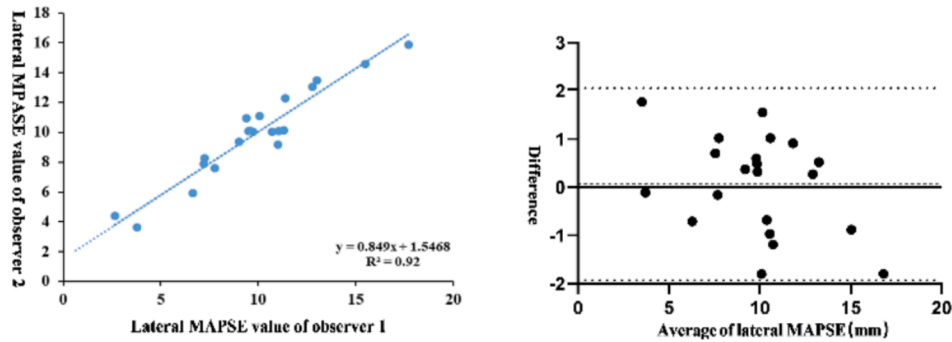


**Fig. 6.** Linear regression (left) and Bland-Altman plots (right) of lateral MAPSE and septal MAPSE for inter-observer variability. In Bland-Altman plots, solid line represented average value, dashed lines represented 95 %limits of agreement.

verified yet. Initial studies found that longitudinal orientation of sub-endocardial myocardial fibers is the dominant contributor to left ventricular ejection fraction (LVEF) [34], while, recent studies declared that the microstructures sheetlets of myocardial, consisting of several myocytes and working together as one mechanical unit, were thought to be a main contributor to systolic myocardial thickening in hypertrophic cardiomyopathy [37]. The similar result also be found in acute ischemic heart disease of a rhesus monkey experiment, which showed a reduction of the number of subendocardial fibers arranging from right-hand, as well as the range of helix angles [38].

In ischemic heart disease, MAPSE obtained by echocardiographic methods was shown to have a high correlation with cardiac events [39,40]. However, studies seemed relatively few by CMRI so far [41–43], besides, studies specifically assessing MAPSE in CAD patients by CMRI have been limited to date. Rangarajan et al previously showed that lateral MAPSE derived from cine image was an independent predictor of cardiac event in an unselected cohort. In contrast to our study, there consecutive patients enrolled from a single center without knowing their coronary information [41]. Another study examined the prognostic value of similarly derived cardiac MR imaging MAPSE from 255 STEMI patients, after a median follow-up of 3 years, they found that MAPSE was the independent predictor of MACE with the AUC = 0.74 and cutoff value = 9 mm [44]. There still exists some differences between the results above and ours. We found the lateral MAPSE other than the septal that contributes to cardiac event, with the cutoff value = 9.88 mm. Given that their MAPSE was defined as the perpendicular distance of the end-systolic mitral annular plane to the end-diastolic plane, while ours was liner distance, which may explain the discrepancy. Besides, the research cohort was different, our patients included significant and non-significant coronary stenosis, theirs only included the STEMI infarction patients who may had a more seriously cardiac function. Based on the significantly higher predictive value as well as the lower variability of lateral compared with lateral in our research, we consider the prognostic value of lateral MAPSE to be reasonable.

MAPSE can be used to assess global long-axis function, but for the assessment of segmental myocardial function, strain analysis may be preferable. Longitudinal strain assessed by specialized CMR techniques such as feature-tracking promised risk stratification in patients with various cardiac disease including ischemic heart disease [45,46]. good imaging quality is an essential prerequisite for strain analysis, in case of poor imaging quality, such as blood motion affecting endocardial region [47], MAPSE is still a suitable choice for assessing longitudinal systolic function. In our study which data was acquired 9 or 10 years ago, the quality of cine image is relatively poor, thus, MAPSE is a more suitable predictor for cardiac events other than strain analysis.

## 5. Limitations

The cine images were acquired in a single 4-chamber view for it was initially scanned for the preparation of CMRA scanning. Thus, LVEF

value was not capable because of lacking short-axis view. However, since all those patients underwent echocardiography exam on hospital admission, we reviewed those data and finally obtained the LVEF based on echocardiography. Besides, previous studies had proved a more inferior prognostic value of LVEF compared with MAPSE41, 42, 44, which were similar to our results. In addition, not all possible imaging variables were measured, such as left atrial function parameters. Future studies may address the left atrium parameters.

This simple measurement methods for MAPSE didn't take into accounts factors such as patient size, heart size, or age which may confound absolute values of mitral annulus plane motion. However, our study proved that this simple measurement had prognostic value and are more suitable to be used in busy clinical workplace.

## 6. Conclusion

This long-term follow-up proved that lateral MAPSE was a reliable and fast assessable parameter in clinical CMR routine, without the need of additional pulse sequences. It was a powerful, independent predictor of MACE at long-term follow-up (9 years) in patients with suspected CAD. Patients with MAPSE  $\geq$  9.885 mm showed a significantly higher MACE-free survival than patients with MAPSE < 9.885 mm. Compared with traditional clinical markers and CMR markers, lateral MAPSE had an incremental prognostic value and can improve NRI especially in patients with significant coronary stenosis in the prediction of MACE.

## CRedit authorship contribution statement

**Chengxi Yan:** Writing – original draft, Methodology. **Ying Chang:** Visualization, Methodology. **FangWu:** . **Minglei Yang:** Methodology. **Shuangfeng Dai:** Resources. **Jiannan Zhang:** Writing – original draft. **Yuelang Zhang:** Writing – review & editing, Conceptualization.

## Declaration of competing interest

The authors declare that they have no known competing financial interests or personal relationships that could have appeared to influence the work reported in this paper.

## References

- [1] U. Ralapanawa, R. Sivakanesan, Epidemiology and the magnitude of coronary artery disease and acute coronary syndrome: a narrative review, *J. Epidemiol. Global Health.* 11 (2) (2021) 169–177, <https://doi.org/10.2991/jegh.k.201217.001>.
- [2] C. Liu, V.A. Ferrari, Y. Han, Cardiovascular magnetic resonance imaging and heart failure, *Curr. Cardiol. Rep.* 23 (4) (2021) 35, <https://doi.org/10.1007/s11886-021-01464-9>.
- [3] Cirin L, Crişan S, Luca CT, et al. Mitral Annular Plane Systolic Excursion (MAPSE): A Review of a Simple and Forgotten Parameter for Assessing Left Ventricle Function. *J Clin Med.* Sep 5 2024;13(17)doi:10.3390/jcm13175265.

- [4] Cirin L, Crişan S, Luca C-T, et al. Mitral Annular Plane Systolic Excursion (MAPSE): A Review of a Simple and Forgotten Parameter for Assessing Left Ventricle Function. 2024;13(17):5265.
- [5] Koseoglu C, Oncel CR, Dagan G, Coner A, Akkaya O. Mitral annular plane systolic excursion (MAPSE) as a predictor of atrial fibrillation development after coronary artery bypass surgery. *Bratisl Lek Listy*. Jul 11 2024;doi:10.4149/blil\_2024\_78.
- [6] N. Ichikawa, Y. Nishizaki, S. Miyazaki, et al., Efficacy of mitral annular velocity as an alternative marker of left ventricular global longitudinal strain to detect the risk of cancer therapy-related cardiac disorders, *e15877*, *Echocardiography* 41 (7) (2024), <https://doi.org/10.1111/echo.15877>.
- [7] N.M.A.W. Sari, A.M. Soesanto, Right ventricular function in mitral stenosis: plays a fundamental role, *J. Echocardiogr.* (2024), <https://doi.org/10.1007/s12574-024-00663-x>.
- [8] G. Magdy, E. Hamdy, T. Elzawawy, M. Ragab, Value of mitral annular plane systolic excursion in the assessment of contractile reserve in patients with ischemic cardiomyopathy before cardiac revascularization, *Indian Heart J.* 70 (3) (2018) 373–378, <https://doi.org/10.1016/j.ihj.2017.11.004>.
- [9] J.P. MacNamara, W.M. Turlington, K.A. Dias, et al., Impaired longitudinal systolic-diastolic coupling and cardiac response to exercise in patients with hypertrophic cardiomyopathy, *e15857*, *Echocardiography* 41 (6) (2024), <https://doi.org/10.1111/echo.15857>.
- [10] Q. Yang, K. Li, X. Liu, et al., 3.0T whole-heart coronary magnetic resonance angiography performed with 32-channel cardiac coils, *Circ. Cardiovasc. Imaging.* 5 (5) (2012) 573–579, <https://doi.org/10.1161/circimaging.112.974972>.
- [11] Gräni C, Eichhorn C, Bière L, et al. Comparison of myocardial fibrosis quantification methods by cardiovascular magnetic resonance imaging for risk stratification of patients with suspected myocarditis. 2019;21(1):14.
- [12] J. Chan, L. Hanekorn, C. Wong, R. Leano, G.Y. Cho, T.H. Marwick, Differentiation of subendocardial and transmural infarction using two-dimensional strain rate imaging to assess short-axis and long-axis myocardial function, *J. Am. Coll. Cardiol.* 48 (10) (2006) 2026–2033, <https://doi.org/10.1016/j.jacc.2006.07.050>.
- [13] Pickering JW, Endre ZH. New Metrics for Assessing Diagnostic Potential of Candidate Biomarkers. *Clin J Am Soc Nephrol.* 7(8):1355-1364.
- [14] M.J. Pencina, R.B. D'Agostino Sr., R.B. D'Agostino Jr., R.S. Vasan, Evaluating the added predictive ability of a new marker: from area under the ROC curve to reclassification and beyond, ; discussion 207–12, *Stat. Med.* 27 (2) (2008) 157–172, <https://doi.org/10.1002/sim.2929>.
- [15] H. Nishiyama, Y. Tanabe, T. Kido, et al., Incremental diagnostic value of whole-heart dynamic computed tomography perfusion imaging for detecting obstructive coronary artery disease, *J. Cardiol.* 73 (5) (2019) 425–431, <https://doi.org/10.1016/j.jjcc.2018.12.006>.
- [16] I. Danad, J. Szymonifka, J.W.R. Twisk, et al., Diagnostic performance of cardiac imaging methods to diagnose ischaemia-causing coronary artery disease when directly compared with fractional flow reserve as a reference standard: a meta-analysis, *Eur. Heart J.* 38 (13) (2017) 991–998, <https://doi.org/10.1093/eurheartj/ehw095>.
- [17] D. Andreini, G. Pontone, S. Mushtaq, et al., A long-term prognostic value of coronary CT angiography in suspected coronary artery disease, *JACC Cardiovasc Imaging.* 5 (7) (2012) 690–701, <https://doi.org/10.1016/j.jcmg.2012.03.009>.
- [18] M.J. Budoff, D. Dowe, J.G. Jollis, et al., Diagnostic performance of 64-multidetector row coronary computed tomographic angiography for evaluation of coronary artery stenosis in individuals without known coronary artery disease: results from the prospective multicenter ACCURACY (Assessment by Coronary Computed Tomographic Angiography of Individuals Undergoing Invasive Coronary Angiography) trial, *J. Am. Coll. Cardiol.* 52 (21) (2008) 1724–1732, <https://doi.org/10.1016/j.jacc.2008.07.031>.
- [19] Y.E. Yoon, K. Kitagawa, S. Kato, et al., Prognostic value of coronary magnetic resonance angiography for prediction of cardiac events in patients with suspected coronary artery disease, *J. Am. Coll. Cardiol.* 60 (22) (2012) 2316–2322, <https://doi.org/10.1016/j.jacc.2012.07.060>.
- [20] Q. Yang, K. Li, X. Liu, et al., Contrast-enhanced whole-heart coronary magnetic resonance angiography at 3.0-T: a comparative study with X-ray angiography in a single center, *J. Am. Coll. Cardiol.* 54 (1) (2009) 69–76, <https://doi.org/10.1016/j.jacc.2009.03.016>.
- [21] H. Sakuma, Y. Ichikawa, S. Chino, T. Hirano, K. Makino, K. Takeda, Detection of coronary artery stenosis with whole-heart coronary magnetic resonance angiography, *J. Am. Coll. Cardiol.* 48 (10) (2006) 1946–1950.
- [22] D. Piccini, P. Monney, C. Sierro, et al., Respiratory self-navigated postcontrast whole-heart coronary MR angiography: initial experience in patients, *Radiology* 270 (2) (2014) 378–386.
- [23] Y.E. Yoon, K. Kitagawa, S. Kato, et al., Prognostic value of coronary magnetic resonance angiography for prediction of cardiac events in patients with suspected coronary artery disease, *J. Am. Coll. Cardiol.* 60 (22) (2016) 2316–2322.
- [24] J.R. Arnold, G.P. McCann, Cardiovascular magnetic resonance: applications and practical considerations for the general cardiologist, *Heart* 106 (3) (2020) 174–181, <https://doi.org/10.1136/heartjnl-2019-314856>.
- [25] T. Nabeta, T. Inomata, Y. Iida, et al., Baseline cardiac magnetic resonance imaging versus baseline endomyocardial biopsy for the prediction of left ventricular reverse remodeling and prognosis in response to therapy in patients with idiopathic dilated cardiomyopathy, *Heart Vessels.* 29 (6) (2014) 784–792, <https://doi.org/10.1007/s00380-013-0415-1>.
- [26] L. Tondi, S. Pica, G. Crimi, et al., Interstitial fibrosis is associated with left atrial remodeling and adverse clinical outcomes in selected low-risk patients with hypertrophic cardiomyopathy, *Int. J. Cardiol.* 408 (2024) 132135, <https://doi.org/10.1016/j.ijcard.2024.132135>.
- [27] Wagner A, Mahrholdt H, Holly TA, et al. Contrast-enhanced MRI and routine single photon emission computed tomography (SPECT) perfusion imaging for detection of subendocardial myocardial infarcts: an imaging study. 2003;361(9355):374-379.
- [28] Selvanayagam JB, Kardos A, Francis JM, et al. Value of delayed-enhancement cardiovascular magnetic resonance imaging in predicting myocardial viability after surgical revascularization. 2005;14(1):28-28.
- [29] P.A. Scott, J.M. Morgan, N. Carroll, et al., The extent of left ventricular scar quantified by late gadolinium enhancement MRI is associated with spontaneous ventricular arrhythmias in patients with coronary artery disease and implantable cardioverter-defibrillators, *Circ. Arrhythm. Electrophysiol.* 4 (3) (2011) 324–330.
- [30] Iles L, Pfluger H, Lefkovits L, et al. Myocardial Fibrosis Predicts Appropriate Device Therapy in Patients With Implantable Cardioverter-Defibrillators for Primary Prevention of Sudden Cardiac Death. 2011;57(7):821-828.
- [31] T.O.M. Spaapen, A.E. Bohte, M.G. Sliker, H.B. Grotenhuis, Cardiac MRI in diagnosis, prognosis, and follow-up of hypertrophic cardiomyopathy in children: current perspectives, *Br. J. Radiol.* 97 (1157) (2024) 875–881, <https://doi.org/10.1093/bjr/tqae033>.
- [32] R.Y. Kwong, H. Sattar, H. Wu, et al., Incidence and prognostic implication of unrecognized myocardial scar characterized by cardiac magnetic resonance in diabetic patients without clinical evidence of myocardial infarction, *Circulation.* 118 (10) (2008) 1011–1020.
- [33] A. Mayr, M. Pampering, M. Reindl, et al., Mitral annular plane systolic excursion by cardiac MR is an easy tool for optimized prognosis assessment in ST-elevation myocardial infarction, *Eur. Radiol.* 30 (1) (2020) 620–629, <https://doi.org/10.1007/s00330-019-06393-4>.
- [34] Carlsson M, Ugander M, Mosén H, Buhre T, Arheden H. Atrioventricular plane displacement is the major contributor to left ventricular pumping in healthy adults, athletes, and patients with dilated cardiomyopathy. 2007;292(3):H1452.
- [35] K. Hu, D. Liu, S. Herrmann, et al., Clinical implication of mitral annular plane systolic excursion for patients with cardiovascular disease, *Eur. Heart J. Cardiovasc. Imaging.* 14 (3) (2013) 205–212.
- [36] Y.H. Wang, L. Sun, S.W. Li, et al., Normal reference values for mitral annular plane systolic excursion by motion-mode and speckle tracking echocardiography: a prospective, multicentre, population-based study, *Eur. Heart J. Cardiovasc. Imaging.* 24 (10) (2023) 1384–1393, <https://doi.org/10.1093/ehjci/jead187>.
- [37] S. Nielles-Vallespin, Z. Khalique, P.F. Ferreira, et al., Assessment of myocardial microstructural dynamics by in vivo diffusion tensor cardiac magnetic resonance, *J Am Coll Cardiol.* 69 (6) (2017) 661–676, <https://doi.org/10.1016/j.jacc.2016.11.051>.
- [38] Y. Wang, W. Cai, L. Wang, R. Xia, Evaluate the early changes of myocardial fibers in rhesus monkey during sub-acute stage of myocardial infarction using diffusion tensor magnetic resonance imaging, *Magn. Reson. Imaging.* 34 (4) (2016) 391–396.
- [39] Berg J, Jablonowski R, Mohammad M, et al. Ventricular longitudinal shortening is an independent predictor of death in heart failure patients with reduced ejection fraction. *Sci Rep.* Oct 13 2021;11(1):20280. doi:10.1038/s41598-021-99613-1.
- [40] M. Ersbøll, N. Valeur, U.M. Mogensen, et al., Prediction of all-cause mortality and heart failure admissions from global left ventricular longitudinal strain in patients with acute myocardial infarction and preserved left ventricular ejection fraction, *J. Am. Coll. Cardiol.* 61 (23) (2013) 2365–2373, <https://doi.org/10.1016/j.jacc.2013.02.061>.
- [41] Rangarajan V, Chacko SJ, Romano S, et al. Left ventricular long axis function assessed during cine-cardiovascular magnetic resonance is an independent predictor of adverse cardiac events *Journal of Cardiovascular Magnetic Resonance.* 2016;18(1):35.
- [42] S. Romano, R.M. Judd, R.J. Kim, et al., Left ventricular long-axis function assessed with cardiac cine mr imaging is an independent predictor of all-cause mortality in patients with reduced ejection fraction: a multicenter study, *Radiology.* 286 (2) (2018) 452–460, <https://doi.org/10.1148/radiol.2017170529>.
- [43] S. Seitler, A.S. De Zoysa, C.C.C. Obiano, et al., Systolic anterior motion of the anterior mitral valve leaflet begins in subclinical hypertrophic cardiomyopathy, *Eur. Heart J. Cardiovasc. Imag.* 25 (1) (2023) 86–94, <https://doi.org/10.1093/ehjci/jead186>.
- [44] A. Mayr, M. Pampering, M. Reindl, S. Greulich, B. Metzler, Mitral annular plane systolic excursion by cardiac MR is an easy tool for optimized prognosis assessment in ST-elevation myocardial infarction, *Eur. Radiol.* 3 (2019).
- [45] Zhang X, Wang C, Huang Y, Zhang SJ, Xu J. Unveiling the Diagnostic Value of Strain Parameters Across All 4 Cardiac Chambers in Patients With Acute Myocarditis With Varied Ejection Fraction: A Cardiovascular Magnetic Resonance Feature-Tracking Approach. *J Am Heart Assoc.* Jul 2 2024;13(13):e032781. doi: 10.1161/jaha.123.032781.
- [46] J. Gavara, J.F. Rodriguez-Palomares, F. Valente, et al., Prognostic value of strain by tissue tracking cardiac magnetic resonance after ST-segment elevation myocardial infarction, *JACC Cardiovasc. Imaging.* 11 (10) (2018) 1448–1457, <https://doi.org/10.1016/j.jcmg.2017.09.017>.
- [47] P.S. Rajiah, K. Kalisz, J. Broncano, et al., Myocardial strain evaluation with cardiovascular mri: physics, principles, and clinical applications, *Radiographics* 42 (4) (2022) 968–990, <https://doi.org/10.1148/rg.210174>.